Clim. Past, 11, 1417–1431, 2015
www.clim-past.net/11/1417/2015/
doi:10.5194/cp-11-1417-2015

Climate of the Past
Open Access
EGU

Increased aridity in southwestern Africa during the warmest periods of the last interglacial

D. H. Urrego[1,2], M. F. Sánchez Goñi[1], A.-L. Daniau[3], S. Lechevrel[4], and V. Hanquiez[4]

[1]Ecole Pratique des Hautes Etudes EPHE, Université de Bordeaux, Environnements et Paléoenvironnements Océaniques et Continentaux (EPOC), Unité Mixte de Recherche 5805, 33615 Pessac, France
[2]Geography, College of Life and Environmental Sciences, University of Exeter, Exeter, UK
[3]Centre National de la Recherche Scientifique CNRS, Université de Bordeaux, Environnements et Paléoenvironnements Océaniques et Continentaux (EPOC), Unité Mixte de Recherche 5805, 33615 Pessac, France
[4]Université de Bordeaux, Environnements et Paléoenvironnements Océaniques et Continentaux (EPOC), Unité Mixte de Recherche 5805, 33615 Pessac, France

Correspondence to: D. H. Urrego (d.urrego@exeter.ac.uk)

Received: 14 December 2014 – Published in Clim. Past Discuss.: 16 February 2015
Accepted: 17 September 2015 – Published: 20 October 2015

Abstract. Terrestrial and marine climatic tracers from marine core MD96-2098 were used to reconstruct glacial–interglacial climate variability in southwestern Africa between 194 and 24 thousand years before present. The pollen record documented three pronounced expansions of Nama-karoo and fine-leaved savanna during the last interglacial (Marine Isotopic Stage 5 – MIS 5). These Nama-karoo and fine-leaved savanna expansions were linked to increased aridity during the three warmest substadials of MIS 5. Enhanced aridity potentially resulted from a combination of reduced Benguela Upwelling, expanded subtropical high-pressure cells, and reduced austral-summer precipitation due to a northward shift of the Intertropical Convergence Zone. Decreased austral-winter precipitation was likely linked to a southern displacement of the westerlies. In contrast, during glacial isotopic stages MIS 6, 4 and 3, fynbos expanded at the expense of Nama-karoo and fine-leaved savanna indicating a relative increase in precipitation probably concentrated during the austral winter months. Our record also suggested that warm–cold or cold–warm transitions between isotopic stages and substages were punctuated by short increases in humidity. Increased aridity during MIS 5e, 5c and 5a warm substages coincided with minima in both precessional index and global ice volume. On the other hand, austral-winter precipitation increases were associated with precession maxima at the time of well-developed Northern Hemisphere ice caps.

1 Introduction

Southern Africa is influenced at present by tropical and subtropical atmospheric circulation and by both the Indian and the Atlantic oceans (Tyson and Preston-Whyte, 2000). The water exchange between the two oceans is termed the Agulhas leakage and is suggested as a potential trigger of meridional overturning circulation changes (Beal et al., 2011; Biastoch et al., 2008). The Benguela Upwelling System (BUS) also affects climate in southwestern Africa and is linked to arid conditions on the continent (Lutjeharms and Meeuwis, 1987). The complex link between globally important atmospheric and oceanic systems and the climate of southern Africa make understanding past climate change in the region particularly significant.

Whether southern Africa was characterised by aridity or by increased humidity during the last interglacial remains unclear. Previous work using planktic foraminifera assemblages has documented an intensification of the Agulhas leakage during interglacials (Peeters et al., 2004), which suggests a reduced influence of the subtropical front and reduced precipitation. Other works have shown increased sea surface temperatures (SSTs) in the Benguela Current during interglacials linked to weakening of BUS (Kirst et al., 1999). Additionally, decreased influence of the Intertropical Convergence Zone (ITCZ) has been suggested for southern Africa during interglacials (Tyson, 1999), pointing to its

northward migration. These three climatic factors combined would result in a slight increase in humidity in northeastern South Africa during interglacials. However, other works suggest contrasting climate conditions with increased interglacial aridity based on ratios of aeolian dust and fluvial mud in marine sediments off southern Africa (Stuut and Lamy, 2004).

Vegetation-based climate reconstructions for southern Africa have been less straightforward given the paucity of records (Dupont, 2011) and fragmentary nature of some terrestrial sequences (Scott et al., 2012; Meadows et al., 2010). On the one hand, some records point to expansions of the fynbos biome (Shi et al., 2001) and the winter-rainfall zone during glacial periods (Chase and Meadows, 2007), and to a contracting Namib Desert during interglacials (Shi et al., 2000) and the late Holocene (Scott et al., 2012). On the other hand, it has been suggested that savannas expanded southwards during the Holocene climate optimum (Dupont, 2011), and that the southern Africa summer-rainfall zone expanded during interglacials due to a strengthening of the Walker circulation and a southward migration of the ITCZ (Tyson, 1999). Contrastingly, significant reductions of austral-summer precipitation in southern Africa are suggested to coincide with precession minima both during glacials and interglacials (Partridge et al., 1997) and are independently supported by reductions of grass-fuelled fires in the subcontinent (Daniau et al., 2013). The latter observations suggest aridity increase and savanna biome reductions, instead of expansions, during the last-interglacial precession minima. Whether the last interglacial was characterised by orbitally driven increased aridity or increased precipitation may have significant implications for resource availability and climate in the region today and in the near future. Projected patterns of precipitation change for the end of the 21st century indicate at least a 20 % reduction in precipitation in southern Africa compared to pre-2005 values (IPCC, 2014). Understanding glacial–interglacial climate and vegetation dynamics in this region may help unravel how much of the projected precipitation change corresponds to natural variability.

In this study we aim to disentangle the contrasting hypotheses of orbital-scale climate change in southern Africa by combining terrestrial and marine tracers from the marine sequence MD96-2098. We use pollen and charcoal as terrestrial tracers, and δ^{18}O from benthic foraminifera as a marine tracer. Vegetation reconstructions from marine records have contributed to our understanding of ocean–land interactions in many regions of the world, including the Iberian Peninsula (Sánchez Goñi et al., 2000), the eastern subtropical Pacific (Lyle et al., 2012), and the tropical Atlantic (González and Dupont, 2009). Studies from the African margin (e.g. Dupont, 2011; Dupont and Behling, 2006; Hooghiemstra et al., 1992; Leroy and Dupont, 1994; Lézine and Hooghiemstra, 1990) have demonstrated that pollen records from marine sequences are reliable and useful tools to reconstruct changes in the regional vegetation of adjacent landmasses and the climate dynamics at orbital and suborbital timescales. In arid environments, marine sequences are particularly essential in providing continuous records of vegetation change at the regional scale.

The pollen sequence from MD96-2098 presented here covers the period between 24 and 190 thousand years before present (ka) and provides an integrated picture of past regional vegetation changes in southwestern Africa. Southwestern Africa refers here to the western half of South Africa and Namibia that is drained by the Orange River. We compare vegetation-based atmospheric changes with independent climatic markers from the same marine sequence, along with other regional records for oceanic conditions and global ice dynamics, to reconstruct atmospheric and oceanic configurations around southern Africa for Marine Isotopic Stages (MIS) 6, 5, 4 and 3.

2 Modern environmental setting

The southwestern part of the African continent (Atlantic side) is influenced by the seasonal migration of the subtropical front and the southern westerlies that bring precipitation during the austral-winter months (Beal et al., 2011). Precipitation in southwestern Africa is additionally controlled by the cold Benguela Current and wind-driven upwelling that results in aridity on the adjacent continent (Stuut and Lamy, 2004). In the Indian Ocean, warm waters from the Agulhas Current (Beal and Bryden, 1999) and austral-summer heat enhance evaporation and result in relatively high precipitation in southeastern Africa and the interior of the continent (Fig. 1). Austral-summer precipitation is also linked to the position of tropical low-pressure systems (e.g. ITCZ) and reduced subtropical high pressure (Tyson and Preston-Whyte, 2000). As tropical low-pressure systems migrate northwards during the austral winter, subtropical high-pressure cells expand and reduce precipitation in southern Africa. This climatic configuration broadly determines the vegetation distribution in southern Africa.

The vegetation of southern Africa was initially classified into phytogeographical regions (White, 1983; Goldblatt, 1978), and later revisited and described into seven biome units (Rutherford, 1997). These include the succulent karoo, Nama-karoo, desert, savanna, fynbos, grassland, and forest (Fig. 1). The succulent karoo receives between 20 and 290 mm yr^{-1}, of which more than 40 % falls during the austral-winter months (Rutherford, 1997). The two most abundant succulent families are Crassulaceae and Mesembryanthemaceae, and non-succulents are Anacardiaceae, Asteraceae, and Fabaceae (Milton et al., 1997). C4 perennial grasses (Poaceae) have relatively low abundance in the succulent karoo (Milton et al., 1997).

The Nama-karoo receives precipitation from 60 to 400 mm yr^{-1}, falling primarily during the austral summer

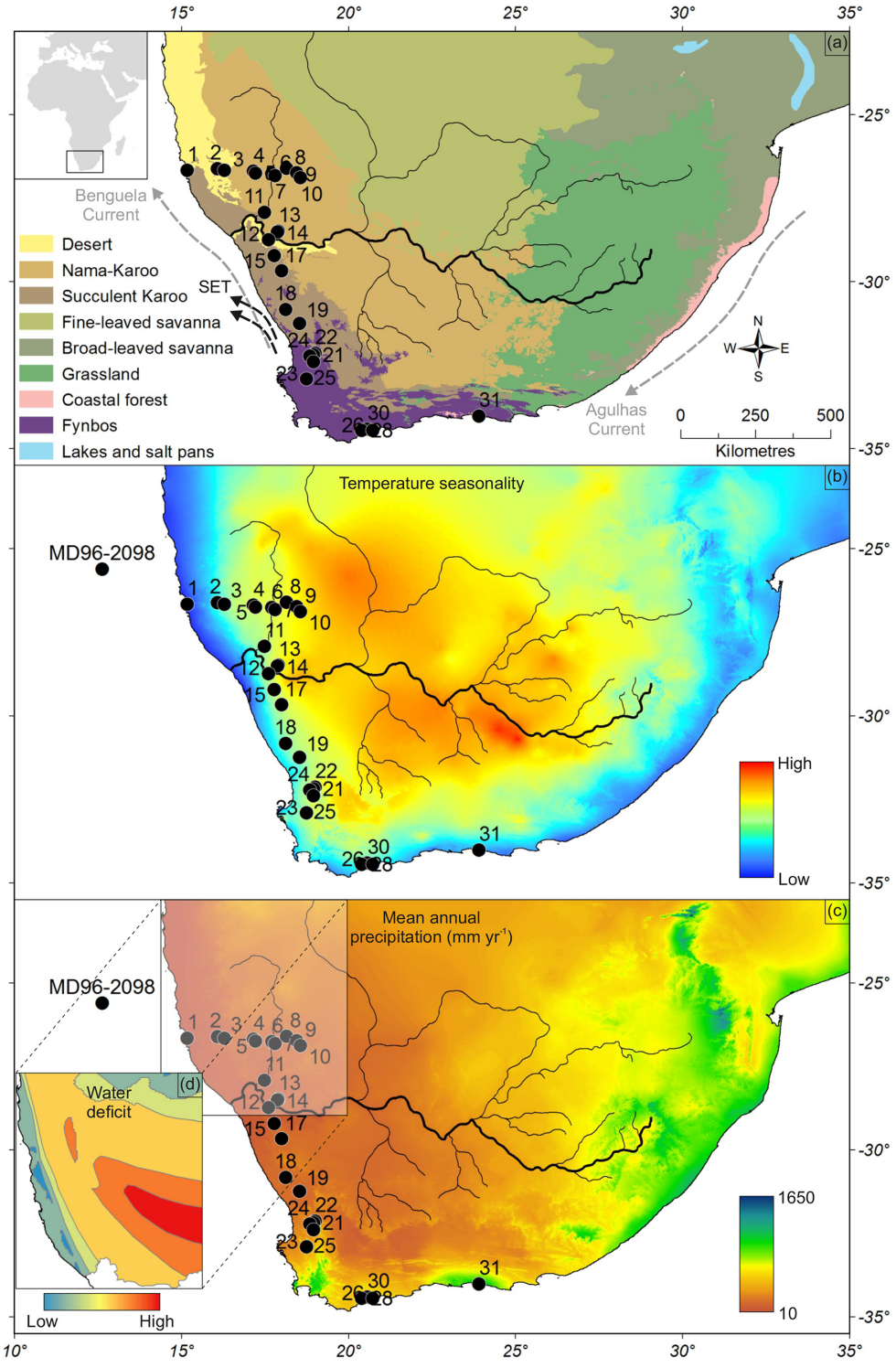

Figure 1. **(a)** Map of biomes of southern Africa based on Mucina et al. (2007) and modified using the savanna classification by Scholes (1997), location of the Orange River and major tributaries, oceanic currents (grey arrows) and southeastern trade winds (black arrows). Temperature seasonality **(b)** and mean annual precipitation in mm yr^{-1} **(c)** extracted from the WorldClim data set (Hijmans et al., 2005). Water deficit data **(d)** redrawn from Barnard (1998) and Digital Atlas of Namibia (http://www.uni-koeln.de/sfb389/e/e1/download/atlas_namibia). Black dots indicate location of marine core MD96-2098 and numbers indicate the location of surface sample collection points described in Table S1 in the Supplement.

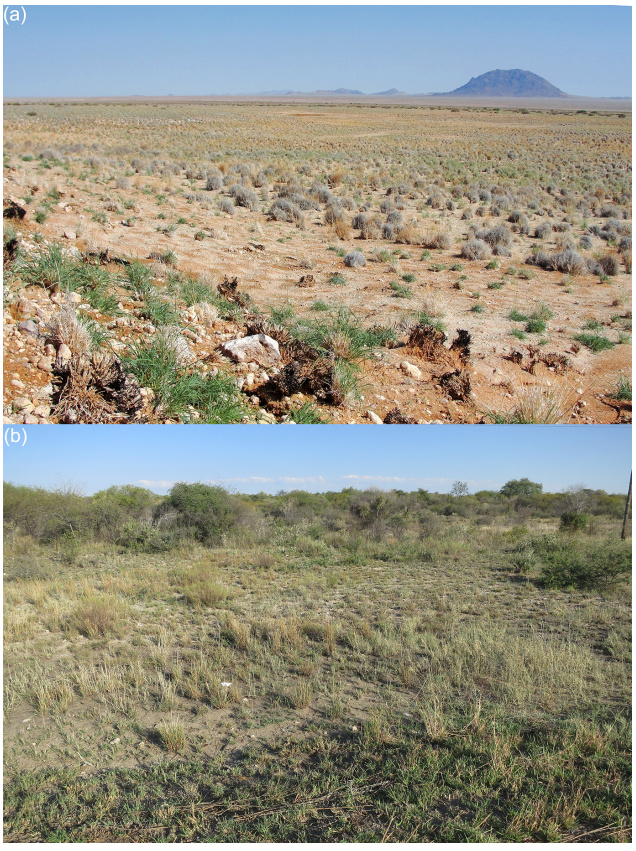

Figure 2. **(a)** Grass-dominated Nama-karoo vegetation near Grunau, Namibia. Photo: D. H. Urrego. **(b)** Grass-dominated fine-leaved savanna vegetation in the Kalahari region of Namibia. Photo: F. d'Errico.

(Palmer and Hoffman, 1997). Vegetation is characterised as dwarf open shrubland with high abundance of Poaceae, Asteraceae, Aizoaceae, Mesembryanthemaceae, Liliaceae and Scrophulariaceae (Palmer and Hoffman, 1997). Grasses from the Poaceae family can be particularly dominant in the Nama-karoo biome (Fig. 2a). The Nama-karoo and succulent karoo are structurally similar but influenced by different seasonal precipitation (Rutherford, 1997). The Nama-karoo is influenced primarily by austral summer precipitation, while the distribution of the succulent karoo coincides with the austral-winter rainfall region (Chase and Meadows, 2007). To the northwest, the Nama-karoo biome transitions into the desert, where mean annual precipitation can be as low as 20 mm yr^{-1} (Jürgens et al., 1997) and water deficit as high as 2000 mm (Barnard, 1998, Fig. 1d). The desert reaches 300 km inland and its low precipitation input is linked to the intensity of BUS (Cowling et al., 1994).

High precipitation seasonality (i.e. difference between dry-season and rainy-season precipitation) and high austral-summer rainfall characterise the savanna. The savanna biome represents a mosaic that includes shrublands, dry forests, lightly wooded grasslands, and deciduous woodlands (Scholes, 1997). At the landscape scale, however, the savanna can be subdivided into the fine- and broad-leaved savannas based on moisture conditions and soils (Scholes, 1997). The fine-leaved savanna (Fn-LSav) is found in fertile and dry environments (between 400 and 800 mm yr^{-1}), and the broad-leaved savanna (Bd-LSav) is found in nutrient-poor and moist environments (up to 1500 mm yr^{-1}) (Scholes, 1997). Additionally, in the Fn-LSav fuel load and fire frequency are very low, while Bd-LSav has high fuel load and fire frequency (Scholes, 1997; Archibald et al., 2010). The Fn-LSav is found to the northeast of the Nama-karoo biome (Fig. 1), known as the Kalahari Highveld transition zone (Cowling and Hilton-Taylor, 2009). Due to the transitional character of the Fn-LSav, some of its outer parts have been classified as grassland or Nama-karoo (White, 1983). The composition of the Fn-LSav can be similar to that of the Nama-karoo, with dominance of C4 grasses (Poaceae) and succulent plants, but it differs in having scattered trees (Fig. 2b) (Cowling et al., 1994). The Bd-LSav is characterised by broad-leaved trees from the Caesalpiniaceae and Combretaceae families and an understory dominated by grasses (Scholes, 1997).

The grassland biome is dominated by C4 grasses and non-grassy forbs as *Anthospermum* sp., *Lycium* sp., *Solanum* sp. and *Pentzia* sp. (O'Connor and Bredenkamp, 1997). At the high elevations the biome is dominated by C3 grasses. In the grasslands, precipitation is highly seasonal with mean annual rainfall ranging between 750 and 1200 mm, falling primarily during the austral-summer months (O'Connor and Bredenkamp, 1997) (Fig. 1).

The southernmost part of Africa is characterised by the fynbos biome, a fire-prone vegetation dominated by Ericaceous and Asteraceae shrubs, diverse *Protea* shrubs and trees, and Restionaceae herbs (Cowling et al., 1997a). This biome receives relatively high annual precipitation (1200 mm per year) concentrated during the austral-winter months (Rutherford, 1997). The coastal forest biome is found along the eastern coast of the subcontinent and often occurs in small patches with high abundance of *Podocarpus* (Rutherford, 1997). *Podocarpus* patches can also be found in the southeastern part of the fynbos.

3 Materials and methods

3.1 Marine core description and pollen analysis

Pollen analysis was conducted on marine core MD96-2098 (25°36′ S, 12°38′ E). This giant CALYPSO core was collected during the IMAGES II-NAUSICAA cruise at a 2910 m water depth from the Lüderitz slope in the Walvis Basin, approximately 500 km northwest of the Orange River mouth (Fig. 1). The sediments of this 32 m long core were composed of calcium carbonates, biogenic silica, clays and organic matter (Bertrand et al., 1996). The core was sampled every 10 cm between 450 and 1940 cm (uncorrected depth) for pollen analysis. The uncorrected depth did not take into account ar-

tificial gaps created during piston extraction (Bertrand et al., 1996).

Sample volumes were estimated by water displacement. Pollen concentrations per unit volume were calculated based on a known spike of exotic *Lycopodium* spores added to each sample. Pollen extraction techniques included treatment with hydrofluoric and hydrochloric acids, and sieving through 150 and 10 µm filters. This filtration allowed for separating small non-palynomorph particles and concentrating pollen grains and spores. An independent test of this protocol showed that the use of a 10 µm sieve had no effect on the pollen spectra of marine samples – i.e. comparison of filtered and unfiltered sample counts showed that taxa were not selectively filtered out during pollen preparation and concentration (see http://www.ephe-paleoclimat.com/ephe/Lab%20Facilities.htm for a detailed pollen preparation protocol). Marine sediment samples from MD96-2098 were analysed under the microscope until a sum of at least 100 pollen grains excluding fern spores was reached.

We used the pollen spectra from 31 terrestrial surface samples collected along a transect (Fig. 1) from Cape Town (South Africa) to Lüderitz (Namibia) and designed to cover the four major biomes of southwestern Africa (Table S1 in the Supplement). The transect included samples from the desert, fynbos, Nama-karoo and succulent karoo. The terrestrial surface samples were treated with standard acetolysis (Faegri and Iversen, 1989) and analysed under the microscope until a pollen sum greater than 300 grains was reached. Additional details on terrestrial surface-sample collection and analysis can be found in the Supplement. We also used previously published pollen spectra from 150 additional surface samples collected between 22 and 35° latitude south (African Pollen Database; Gajewski et al., 2002). These pollen spectra were used to assess the distribution of Poaceae pollen abundance and other pollen taxa with potential indicator value for large biomes in southern Africa. ArcGIS 10 was used to draw isolines of pollen percentages by interpolating values from a total of 178 surface samples through the natural neighbour method. Additionally, we analysed two marine pollen samples from the upper part of core MD96-2098 (at 5 and 10 cm depth). We compared the pollen spectra from these core-top samples with the pollen signal of the modern vegetation to evaluate how well marine sediments represent the vegetation of the adjacent landmasses, and to aid interpretation of the pollen record (see also Lézine and Hooghiemstra, 1990).

Pollen identification was aided by the pollen reference collection of the Department of Plant Sciences at the University of the Free State (Bloemfontein, South Africa), the African Pollen Database (http://medias3.mediasfrance.org/pollen), the Universal Pollen Collection (http://www.palyno.org/pollen), and pollen descriptions published by Scott (1982). Pollen grains from the Asteraceae family were grouped into three pollen taxa: *Artemisia*-type, *Stoebe*-type and other morphotypes were classified into Asteraceae-other. Some morphotypes were grouped into family types: Acanthaceae, Chenopodiaceae–Amaranthaceae, Crassulaceae, Cyperaceae, Ericaceae, Myrtaceae, Ranunculaceae, Restionaceae, and Solanaceae.

Detrended correspondence analysis (DCA) and non-metric multidimensional scaling (NMDS) (McCune and Grace, 2002) were used as parametric and non-parametric ordinations to summarise changes in the fossil pollen record. Results from the DCA ordination were preferred when NMDS was unable to reach a stable solution after several random starts, and when stress levels were too high to allow a meaningful interpretation (McCune and Grace, 2002). These ordinations were performed on the complete data set and filtering out pollen morphotypes that occurred only in one sample. Results from the ordination performed on the reduced data set were preferred when differences in axis scores were not discernible between the two ordinations aiming to reduce the statistical effect of rare taxa.

3.2 Marine core chronology

Two sediment gaps between 693 and 709 cm and 759 and 908 cm were described in the core log. These gaps were considered artificial and linked to piston extraction (Bertrand et al., 1996); thus the record could be assumed continuous. Depths were corrected to take into account these artificial sediment gaps. An age model was established for the record based on 16 marine isotope events (MIEs) from the *Cibicidoides wuellerstorfi* δ^{18}O benthic record of MD96-2098 (Bertrand et al., 2002) and 14 accelerator mass spectrometer radiocarbon ages (AMS ^{14}C) from mixed planktonic foraminifera extracted from MD96-2098 (Table S2 in the Supplement). The 14 AMS ^{14}C dates were produced at the Laboratoire de Mesure du Carbone 14. One single ^{14}C date showed an age reversal and was therefore excluded from the chronology on the principle of parsimony. AMS ^{14}C ages were calibrated using the marine09.14c curve (Hughen et al., 2004) from CALIB REV5.0 (Reimer et al., 2013). We applied a 400-year global reservoir correction factor and a weighted mean ΔR of 157 years derived from nine regional reservoir error values from the Marine Reservoir Correction Dataset (Dewar et al., 2012; Southon et al., 2002). MIE ages were derived from LR04 global stack (Lisiecki and Raymo, 2005) and additional sources (Henderson and Slowey, 2000; Drysdale et al., 2007; Waelbroeck et al., 2008; Masson-Delmotte et al., 2010; Sánchez Goñi and Harrison, 2010) (Fig. S1 in the Supplement). Sample ages were calculated using a linear interpolation between AMS ^{14}C ages and MIE using the R package PaleoMAS (Correa-Metrio et al., 2010). The average sedimentation rate of core MD96-2098 amounts to 0.01 cm yr^{-1}.

4 Results and discussion

4.1 Pollen preservation and sources in marine core MD96-2098

Pollen sums ranged from 100 to 240 grains (excluding fern spores) in the 141 samples analysed from core MD96-2098. We identified 83 different pollen taxa in the whole sequence, and the mean number of pollen taxa per sample was 21. The proportion of unknown pollen taxa was between 1 and 2 % per sample. The total pollen concentration ranged between ca. 300 and 16 000 grains cm^{-3} during most of MIS 6, 5 and 3 and increased up to 48 000 grains cm^{-3} during MIS 4 (Fig. S2 in the Supplement). The MIS 5 pollen concentrations were comparable to those found in other oceanic margins (Sánchez Goñi et al., 1999), even though BUS facilitates preservation of pollen grains and other organic microfossils at this site (Bertrand et al., 2003). The low net primary productivity that characterises the vegetation of southwestern Africa (Imhoff et al., 2004) is probably linked to low pollen production and could explain relatively low pollen concentrations in the continental margin (Fig. S2).

Pollen grains are part of the fine sediment fraction and can be transported by two main vectors: aeolian or fluvial (Hooghiemstra et al., 1986; Heusser and Balsam, 1977). Dupont and Wyputta (2003) modelled present-day wind trajectories for marine core locations between 6 and 30° S along the coastline of southern Africa. They suggest aeolian pollen input to the Walvis area (23° S) via the southeast trade winds during austral summer, and dominant east-to-west wind directions during the austral autumn and winter. These winds transport pollen and other terrestrial particles from the Namib Desert, southern Namibia and western South Africa. The direction of the winds indicate that the Namib Desert, Nama-karoo and succulent karoo are the most likely sources of pollen in the Walvis Bay area (Dupont and Wyputta, 2003). The authors also infer that wind directions south of 25° S are predominantly west to east and aeolian terrestrial input is very low. Marine site MD96-2098 is located less than a degree south of the area determined by Dupont and Wyputta (2003) to be dominated by wind-transported terrestrial input. However, given that this threshold was established using only two marine sites located 6° apart at 23°26′ (GeoB1710-3) and 29°27′ (GeoB1722-1), it is difficult to conclude that MD96-2098 only receives wind-transported pollen.

MD96-2098 likely receives fine sediments from the Orange River plume. Sedimentological analyses of the Orange River delta and plume indicate that fine muds are transported both northwards and southwards (Rogers and Rau, 2006). Additionally, an analysis of the imprint of terrigenous input in Atlantic surface sediments found relatively high Fe/K values along the Namibian and South African margin that could reflect the input of Orange River material (Govin et al., 2012). Pollen grains are hence likely to reach the coring site from the Orange River catchment area.

Scott et al. (2004) argue that pollen in marine sediments can be the result of long-distance transport by ocean currents, suggesting that pollen assemblages in marine sediments do not reflect accurately past changes in vegetation and climate. However, the highest pollen influx in marine sediments along this margin is near the coast and the vegetation source (Dupont et al., 2007), not along the paths of oceanic currents (i.e. the Benguela Current). Additionally, analyses of pollen transport vs. source in northwestern Africa show that pollen grains can sink rapidly in the water column (Hooghiemstra et al., 1986) before they can be carried away by ocean currents. As a result, influence of oceanic currents on the composition of pollen assemblages is probably negligible. Overall, the marine site MD96-2098 might receive both aeolian and fluvial pollen input from the vegetation located east and southeast to the site.

The pollen spectra of the two core-top samples from core MD96-2098 are dominated by Poaceae (30 and 40 %), Cyperaceae (20 %) and Chenopodiaceae–Amaranthaceae (20 and 30 %) (Fig. S2 in the Supplement). This composition corresponds well with the pollen spectra from the three major biomes occupying today the adjacent landmasses (Fig. 1a): desert, Nama-karoo and Fn-LSav (Fig. S3 in the Supplement). Pollen percentages from fynbos taxa are less than 10 %, *Podocarpus* is weakly represented, and taxa specifically found in the broad-leaved savanna (e.g. Caesalpiniaceae, Combretaceae) are not recorded. These results support the assumption that the main pollen source for marine core MD96-2098 is the vegetation from southwestern Africa.

4.2 Distribution and interpretation of Poaceae pollen in terrestrial and marine surface samples

Occurrence of Poaceae pollen in all surface samples corresponds to the presence of grass species in virtually all southern African biomes (Cowling et al., 1997b). Altogether, the spatial distribution of Poaceae pollen percentages appears to be essential information to distinguish the pollen signal from major biomes, and therefore climatic zones, in this region. In the eastern and northeastern part of southern Africa, the highest percentages of Poaceae pollen (up to 90 %) are found in the pollen rain of the Bd-LSav and grasslands. In the western half of southern Africa, Poaceae pollen percentages in terrestrial surface samples are up to 60 % in the Nama-karoo and its transition with the Fn-LSav (Fig. 3). This suggests an over-representation of Poaceae in the pollen rain of the Nama-karoo biome, where grasses can be abundant but are not necessarily dominant.

Poaceae is likely to be well represented in other parts of the Fn-LSav, but the paucity of surface samples from this biome hinders the drawing of further conclusions. In the Namib Desert, where the proportion of grasses in the vegetation is low, Poaceae pollen percentages are as high as 25 % in terrestrial surface samples, comparable to 20 % reported from hyrax dung (Scott et al., 2004).

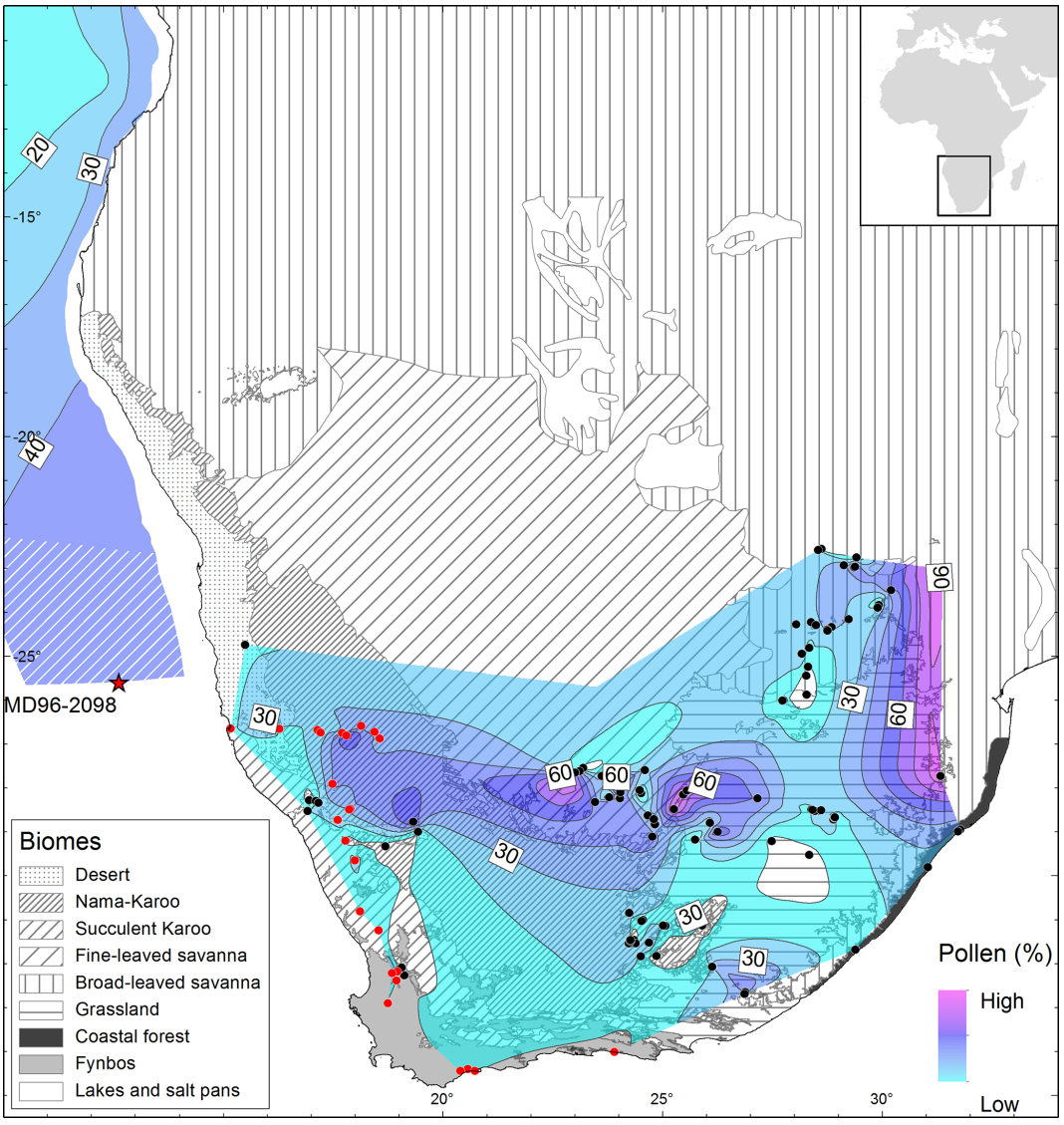

Figure 3. Poaceae pollen percentage isolines drawn over biome units of southern Africa (modified from Scholes, 1997; Mucina et al., 2007). The broad-leaved savanna distribution includes the Mopane and mixed savannas described by Scholes (1997). Isolines are plotted based on pollen percentage data from surface samples analysed in this study (red dots) and pollen spectra from other samples previously published and extracted from the African Pollen Database (black dots) (Gajewski et al., 2002). Poaceae pollen percentages in the marine domain are redrawn from Dupont and Wyputta (2003) and extended to latitude 25° S using two MD96-2098 core-top samples (hatched).

In marine surface samples along the southwestern African coast, Poaceae pollen percentages are as low as 10 % in samples collected offshore of the Bd-LSav at around 15° S (Fig. 3). Poaceae pollen percentages increase to the south and the highest values (40 %) are found between 20 and 25° S (Dupont and Wyputta, 2003) and correspond well with the distribution of the desert and the Fn-LSav on the continent. The Poaceae pollen percentages in the two core-top samples from MD96-2098 are used to extend the isolines drawn by Dupont and Wyputta (2003) to 25.5° S, and show that Poaceae pollen percentages are between 30 and 40 % offshore of the desert, Nama-karoo and Fn-LSav biomes. As Poaceae pollen percentages in desert surface samples are less than 25 %, high percentages of grass pollen from marine sediments in the southwestern Africa margin should be interpreted as an indicator of the Nama-karoo and the Fn-LSav, where Poaceae is as high as 70 % in terrestrial surface samples. Our field observations also support this view as we found large grass-dominated vegetation in the Nama-karoo and Fn-LSav (Fig. 2).

4.3 Southwestern Africa vegetation and climatic changes from MIS 6 to 2

The pollen record presented here spans from 24.7 to 190 ka. A log transformation of concentration values in MD96-2098 results in a curve remarkably similar to that of $\delta^{18}O_{benthic}$ values (Fig. 4) and may be linked to changes in pollen input at the coring site. Relative increases in pollen concentration could indicate an increase in pollen supply during low sea-level stands when the vegetation source was closest (i.e. during glacial stages). However, this is unlikely because of the rapid depth change of the Walvis continental shelf. An increase in pollen concentration might indicate instead an increase in pollen supply during glacials, and/or an increase in pollen preservation linked to upwelling enhancement as suggested by Pichevin et al. (2005). Glacial–interglacial pollen concentration variations have no effect on the interpretation of the pollen record, which is based on relative frequencies, but they do indicate the influence of the obliquity signal in the pollen record from MD96-2098. In other words, the effect of orbital-scale precipitation changes on the density of the vegetation and the pollen production as a consequence.

The axis scores on DCA1 reveal changes in the composition of pollen assemblages that also resemble variations in the $\delta^{18}O_{benthic}$ record (Fig. 4). This similarity suggests that glacial–interglacial vegetation changes in southern Africa track global ice volume changes. DCA1 axis scores from MIS 5 and 3 are overall positive in value, while scores from MIS 6 and 4 are negative, although clustering of samples was not observed. The DCA1 axis represents relative changes in the pollen assemblage from one sample to the next. A series of large-magnitude changes in DCA1 axis scores are also visible and increase in amplitude after ca. 100 ka. Such changes are also observed during MIS 6 but are of lesser magnitude. Changes in DCA axis scores suggest significant changes in vegetation composition from one sample to the next.

Nama-karoo and Fn-LSav pollen percentages are up to 60 % during MIS 5 and display three percentage peaks that correspond with $\delta^{18}O_{benthic}$ and precession minima (Fig. 4a). These percentage peaks are centred at 125, 107 and 83 ka. The pollen spectra from warm marine substages MIS 5e, 5c and 5a are comparable to the core-top samples (Fig. 4) and correspond well with the modern pollen spectra from Nama-karoo and Fn-LSav (Fig. S3 in the Supplement). Additionally, Nama-karoo and Fn-LSav pollen percentages in the core-top samples are relatively low compared to their maximum during MIS 5e (Fig. 4b).

During MIS 6 and 4, Nama-karoo and Fn-LSav percentages are reduced and co-vary with $\delta^{18}O_{benthic}$ values. Pollen percentages of Chenopodiaceae–Amaranthaceae and Asteraceae-other are relatively high and increase along with enriched $\delta^{18}O_{benthic}$ values during MIS 6 and at the end of MIS 4 (Fig. S2). Cyperaceae pollen percentages vary throughout the record and are as high as 40 % during MIS 4 (Fig. S2). Fynbos indicators (Ericaceae, *Passerina*, *Anthospermum*, *Cliffortia*, *Protea*, *Artemisia*-type, and *Stoebe*-type) show relative increases in pollen percentage during MIS 6, 4 and 3 (Figs. 4b and S2). Pollen percentages of Restionaceae increase after the 105 ka $\delta^{18}O_{benthic}$ minimum and remain abundant during the rest of MIS 5 through MIS 3, despite a relative decrease during MIS 4. *Podocarpus* percentages are lower than 10 % but show increases at stage boundaries around 135 ka (MIS 6/5), 100 ka (5c/5b), 75 ka (MIS 5a/4), 60 ka (MIS 4/3), and 27 ka (MIS 3/2) (Fig. S2).

The increases in Nama-karoo and Fn-LSav during MIS 5e, 5c and 5a suggest an increase in aridity in southwestern Africa that likely resulted from expansions in three directions (Fig. 5). The Nama-karoo and Fn-LSav probably expanded to the northwest into the present-day area of the coastal Namib Desert as the intensity of BUS weakened during MIS 5 warm substages. This weakening has been documented through alkenone-based SST from marine core GeoB1711-3 (Kirst et al., 1999) (Fig. 4c), foraminifera-assemblage-based SST (Chen et al., 2002) and grain-size end-member modelling (Stuut et al., 2002). Stuut and Lamy (2004) also suggested reduced atmospheric circulation and weakening of trade winds during interglacials compared to glacials, resulting in a reduction in the wind-driven upwelling. A weakened BUS and the associated relative increase in humidity likely led to a colonisation of desert areas by Nama-karoo or Fn-LSav (Fig. 5a). Comparable contractions of the Namib Desert linked to increased SSTs and weakening of BUS during the present interglacial are documented by Shi et al. (2000).

To the south, the Nama-karoo and Fn-LSav likely expanded at the expense of the succulent karoo and fynbos. Warm Antarctic temperatures recorded during MIS 5 substages (EPICA, 2006) would drive the southern westerlies southwards (Ruddiman, 2006), contributing to the ventilation of deep CO_2-rich waters in the Southern Ocean (Toggweiler and Russell, 2008). This mechanism would explain the paralleling trends observed between MIS 5 Nama-karoo and Fn-LSav expansions in southern Africa and the atmospheric CO_2 record (Petit et al., 1999; Bereiter et al., 2012) (Fig. 5). A southward migration of the westerlies during the present interglacial, relative to their position during the previous glacial, has been suggested by Weldeab et al. (2013), and correlated with non-sea-salt calcium flux ($nssCa^{2+}$) from Antarctica (Röthlisberger et al., 2008). Such poleward migration of the westerlies during the present interglacial is equivalent to the westerlies migration we propose for warmest periods of the last interglacial. The increased Agulhas leakage documented in the Cape Basin record during the last interglacial (Peeters et al., 2004) (Fig. 4c) has been linked to a southward migration of the subtropical front and the westerlies, reducing austral-winter precipitation over southern Africa. Such an atmospheric configuration would in turn favour the development of the Nama-karoo at the expense of succulent karoo and fynbos biomes (Fig. 5a).

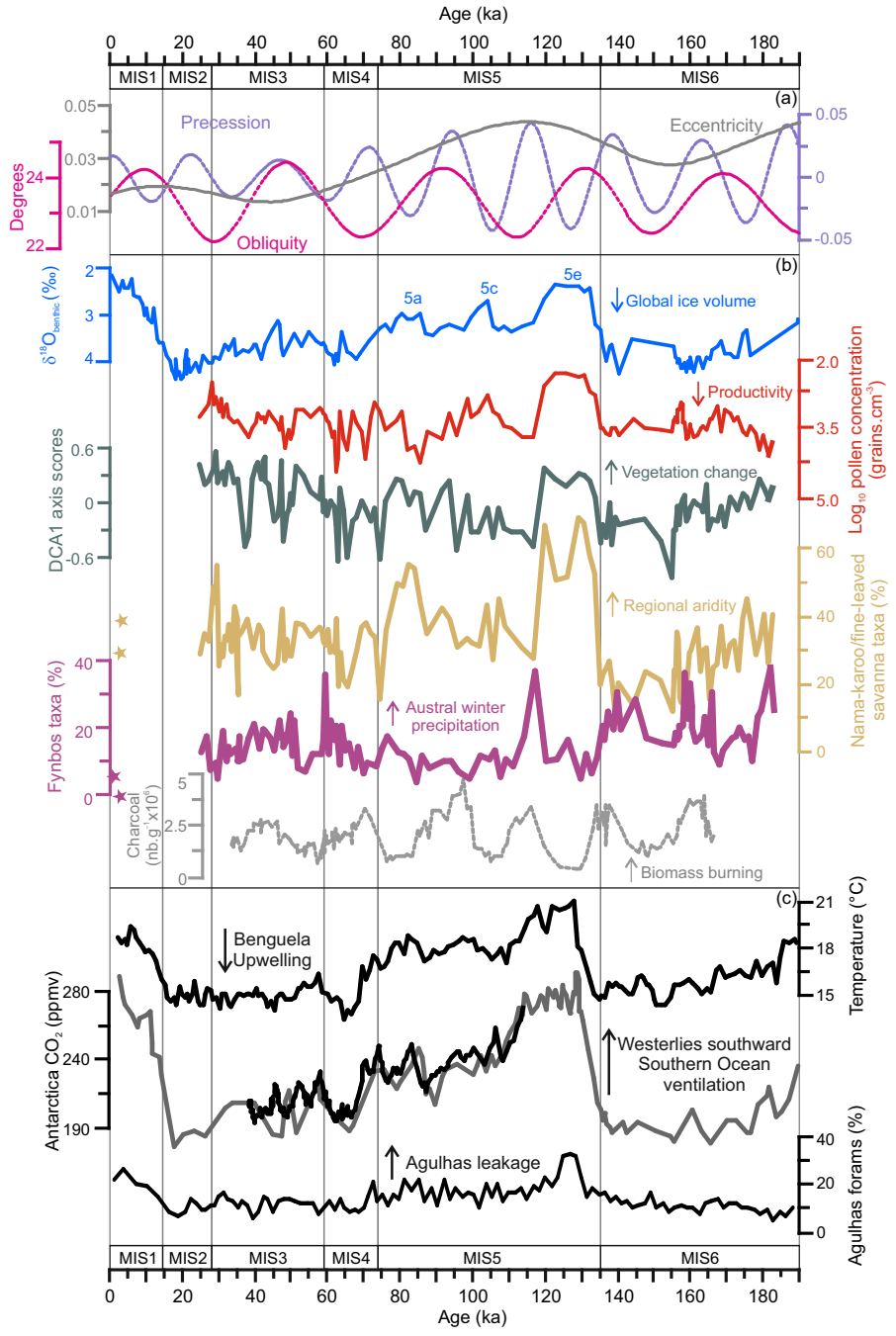

Figure 4. Terrestrial, atmospheric and oceanic markers from southern Africa plotted against age in ka (thousands of calibrated/calendar years before present). **(a)** Orbital parameters plotted for latitude 25°36′ S using La2004 (Laskar et al., 2004). **(b)** Stable oxygen profile of benthic foraminifera *Cibicidoides wuellerstorfi* (Bertrand et al., 2002), log-transformed total pollen concentration plotted on a descending scale, detrended correspondence analysis Axis1 scores, pollen percentages of indicator taxa for Nama-karoo and fine-leaved savanna (Acanthaceae, Aizoaceae, Crassulaceae, Euphorbia, Poaceae, and *Tribulus*), and fynbos (*Artemisia*-type, Ericaceae, *Passerina*, *Protea*, and *Stoebe*-type), charcoal concentrations in number of particles per gram ($nb\,g^{-1}$) from marine core MD96-2098 (Daniau et al., 2013). Stars on the left correspond to percentage of pollen taxa in two top-core samples dating 530 and 1060 calibrated years before present. **(c)** Independent climatic records discussed in the text: alkenone-based SST record from GeoB1711-3 indicating the strength of the Benguela Upwelling system (Kirst et al., 1999). Antarctica CO_2 concentration record; grey curve: low-resolution record from Vostok (Petit et al., 1999); black curve: high-resolution EDML-Talos Dome Antarctic ice core CO_2 data (Bereiter et al., 2012). Cape Basin spliced record of planktic foraminifera assemblages indicating the strength of the Agulhas leakage (Peeters et al., 2004). Stage boundary ages for 3/2, 4/3, and 5/4 from (Sanchez Goñi and Harrison, 2010) and 6/5 from (Henderson and Slowey, 2000).

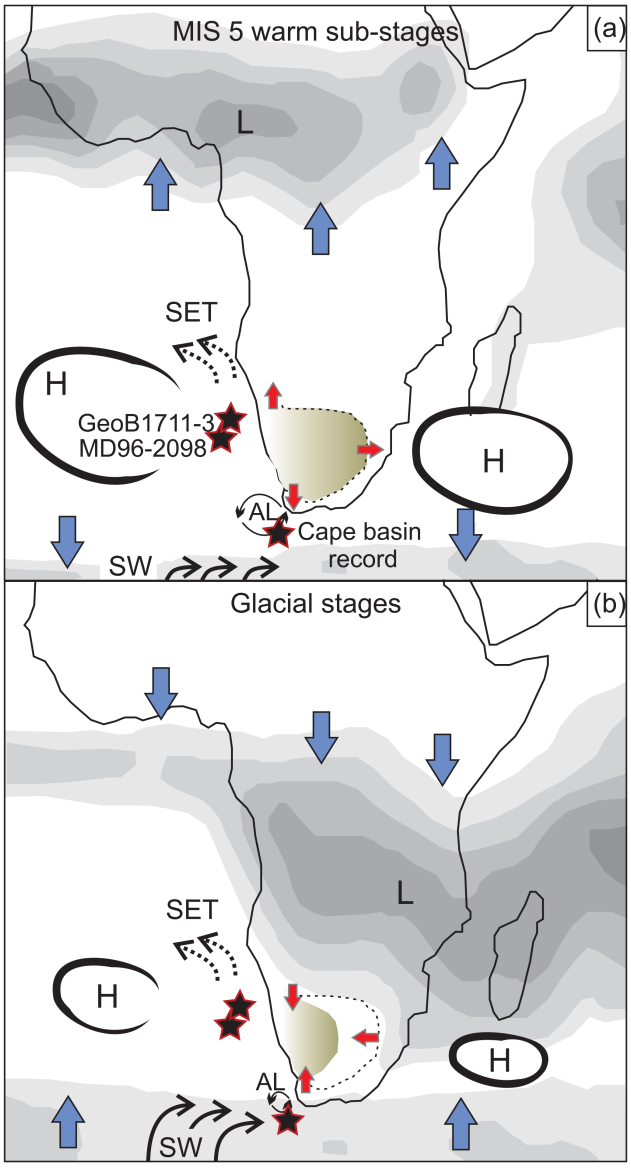

Figure 5. Schematic and simplified configuration of vegetation and atmospheric and oceanic systems over southern Africa during **(a)** the MIS 5 warm substages and **(b)** glacial isotopic stages. Rainfall is illustrated as grey areas showing the current configuration of tropical and subtropical convection systems using average austral-winter **(a)** and austral-summer **(b)** precipitation data between 1979 and 1995 from the International Research Institute for Climate Prediction (http://iri.ldeo.columbia.edu). L: tropical low-pressure systems; H: subtropical high-pressure systems; SET: southeast trade winds; SW: southern westerlies; AL: Agulhas leakage. Stars indicate the location of marine records discussed in the text and blue arrows indicate the direction of pressure system migration. Red arrows and the brown shaded area indicate hypothesised expansion **(a)** or contraction **(b)** of the Nama-karoo and fine-leaved savanna.

To the northeast, Nama-karoo and Fn-LSav likely pushed the limit of Bd-LSav equatorward as austral-summer precipitation decreased (Fig. 5a). Austral-summer precipitation reductions in southern Africa have been linked to reduced austral-summer insolation in the Pretoria saltpan (Partridge et al., 1997) and to reductions of grass-fuelled fires during precession minima reconstructed from MD96-2098 (Daniau et al., 2013) (Fig. 4b). Increased Northern Hemisphere insolation during MIS 5 warm substages would drive the ITCZ northwards while subtropical high-pressure cells over the south Atlantic and the Indian Oceans would expand (Fig. 5a) (Ruddiman, 2006). Such changes in the tropical and subtropical pressure systems would allow the expansion of the Nama-karoo and Fn-LSav to the northeast.

In contrast with the results presented here, previous works report poleward interglacial expansions of savannas based on pollen records from marine sediments along the southwestern African coast (Dupont, 2011). These studies univocally interpret the Poaceae pollen percentage increases as the result of savanna expansions. Such an interpretation is potentially plausible in marine records collecting pollen from broad-leaved savanna vegetation, e.g. the Limpopo Basin (Dupont, 2011). However, our results show that Poaceae pollen percentage increases in sequences located off the southwestern African coast can alternatively indicate the expansion of fine-leaved savanna and Nama-karoo vegetation. Previous studies, on the other hand, do not differentiate between the Bd-LSav and Fn-LSav, despite the significant climatic and structural differences between these two types of vegetation. The Bd-LSav is influenced by fire and receives a considerable amount of precipitation during the austral summer (Scholes, 1997). The Fn-LSav is structurally and climatically more similar to the Nama-karoo biome, as it receives very low austral-summer precipitation and does not burn (Archibald et al., 2010) despite being under a regime of significant precipitation seasonality (Scholes, 1997). If high Poaceae pollen percentages during MIS 5 warm substages in our record were related to expansions of the Bd-LSav and increased summer precipitation, the fire activity should also increase during these substages. Instead, an independent charcoal record from the same marine sequence MD96-2098 (Fig. 4b) documents reductions of grass-fuelled fires and a decrease in austral-summer precipitation during MIS 5 precession minima (Daniau et al., 2013). An atmospheric configuration with reduced austral summer precipitation in southern Africa and the ITCZ shifted northward during the warmest periods of MIS 5 is also consistent with documented strengthening of the Asian monsoon and weakening of the South American monsoon during the last-interglacial precession minima (Wang et al., 2004).

Our results suggest that the Bd-LSav retreated equatorwards during MIS 5 precession minima, while Nama-karoo and Fn-LSav expanded. Nama-karoo and Fn-LSav probably covered a surface area larger than at present during MIS 5 warm substages, as indicated by up to 70 % pollen from this

biome during MIS 5 compared to 35 % in the core-top samples. Recent model experiments on the impact of precession changes on southern African vegetation indicate that high precession is linked to reductions of the Bd-LSav (Woillez et al., 2014). Altogether these vegetation changes point to increased aridity in southwestern Africa during the warmest periods of the last interglacial.

During glacial isotopic stages, contractions of the Nama-karoo and Fn-LSav would result from a different atmospheric configuration (Fig. 5b): a southward migration of the ITCZ and the associated African monsoon (Daniau et al., 2013; Partridge et al., 1997) increasing austral-summer rainfall over southern Africa; an intensification of BUS and decreased SST off the Namibian coast (Stuut and Lamy, 2004; Kirst et al., 1999) leading to aridification of coastal areas; and, lastly, an equatorward migration of the westerlies increasing austral-winter precipitation and allowing a northward expansion of the winter-rain zone in southern Africa (Chase and Meadows, 2007). The proposed glacial precipitation changes are consistent with recent estimates of Last Glacial Maximum palaeoprecipitation based on glacier reconstruction and mass-balance modelling (Mills et al., 2012), with leaf-wax reconstructions of hydroclimate (Collins et al., 2014), and with simulated glacial climatic fluctuations in southern Africa (Huntley et al., 2014).

The pollen record from MD96-2098 also suggested glacial expansions of fynbos (Fig. 4b), as pollen percentages of *Artemisia*-type, *Stoebe*-type, *Passerina* and Ericaceae were higher during MIS 6, 4 and 3 than in the core-top samples (Fig. S2 in the Supplement). These results were consistent with glacial northward expansions of fynbos documented in other pollen records from southern Africa (Shi et al., 2000; Dupont et al., 2007). Our record also documented a large peak in fynbos indicators (Fig. 4b) that coincided with a fast decrease in Nama-karoo and fine-leaved savanna pollen percentages at the MIS 5e–5d transition (ca. 117 ka), a precession and eccentricity maxima (Laskar, 1990), and an accelerated cooling in Antarctica (EPICA, 2006; Masson-Delmotte et al., 2010) (Fig. 4c). As pollen percentages of *Artemisia*-type obtained from surface samples were associated with the fynbos biome and austral-winter precipitation (Figs. S4 and S5 in the Supplement), it cannot be discarded that this peak resulted from a rapid and short-lived expansion of the winter-rain zone of southern Africa. Transitions MIS 6/5 and 4/3 were characterised by small but rapid increases in *Podocarpus*, potentially linked to a short increase in annual precipitation. Such increases in *Podocarpus* have also been documented in other records from southern Africa (Dupont, 2011).

Finally, the amplitude of millennial-scale vegetation changes increased between ca. 100 and ca. 25 ka and was highlighted by switches from negative to positive DCA1 scores (Fig. 4b) and increased variability of Restionaceae pollen percentages. Increased Restionaceae pollen could indicate expansions of fynbos vegetation, or enhanced pollen transport from the fynbos region linked to increased trade-wind strength (see additional discussion on present-day pollen–vegetation–climate relationships in the Supplement). Other fynbos indicators did not display the same trend (Fig. 4), suggesting that Restionaceae variability between 100 and 24 ka was more likely the result of enhanced variability of southeast trade winds. Restionaceae pollen percentage data from a record 2° of latitude north of our marine site also showed comparable increases in the amplitude of millennial-scale changes (Shi et al., 2001). Grain-size wind strength tracers from the Walvis Ridge also displayed enhanced millennial-scale variability, although only after ca. 80 ka (Stuut and Lamy, 2004). An analysis of BUS dynamics over the past 190 ka found increased millennial-scale variability in wind strength after ca. 100 ka and the highest wind strength in this zone during MIS 4 and 3 (Stuut et al., 2002). Such millennial-scale atmospheric reorganisations were probably recorded in the pollen-based DCA analysis as rapid biome shifts in southwestern Africa.

5 Conclusions

Terrestrial and marine markers from the marine core MD96-2098 documented expansions of the Nama-karoo and fine-leaved savanna during MIS 5e, 5c and 5a warm substages. Northwestern expansions of the Nama-karoo and Fn-LSav are potentially linked to the reduction in BUS and a local increase in humidity in the desert area, while aridification increased at a regional scale. Towards the east, Nama-karoo and Fn-LSav expansions probably resulted from increased subtropical high pressure, a northward shift of the ITCZ, and reduced austral-summer precipitation. Nama-karoo and Fn-LSav expansions to the southern boundary are possibly associated with southern displacement of the westerlies and the subtropical front, decreasing austral-winter precipitation.

During glacial isotopic stages MIS 6, 4 and 3, fynbos biome expansions are probably linked to the increased influence of the southern westerlies and austral-winter precipitation in southwestern Africa. Our pollen record also suggested that warm–cold or cold–warm transitions between isotopic stages and substages were punctuated by short increases in humidity. Increased variability in vegetation changes at millennial timescales ca. 100 ka was also documented and could be associated with previously identified enhanced variability of the southeastern trade winds.

Interglacial–glacial southern Africa biome dynamics were linked to atmospheric and oceanic dynamics resulting from changes in global ice volume and precession at orbital timescales. Atmospheric configurations with westerly winds shifted southwards relative to today have been suggested for other interglacials (Peeters et al., 2004) and are projected for the end of the 21st century under current global warming (Beal et al., 2011). This is likely to reduce austral-winter precipitation over southern Africa and favour expansions of the

Nama-karoo at the expense of the winter-rain fed fynbos and succulent karoo biomes. However, taking the current orbital configuration alone, the Nama-karoo and fine-leaved savanna in southern Africa might naturally remain relatively reduced for several millennial ahead.

The Supplement related to this article is available online at doi:10.5194/cp-11-1417-2015-supplement.

Acknowledgements. We would like to thank H. Hooghiemstra and C. Miller for their helpful and constructive feedback. We are also grateful to L. Scott for giving us access to the pollen reference collection at the University of the Free State, Bloemfontein, South Africa. Thanks to K. Gajewski and the African Pollen Database for complementary terrestrial surface data. We acknowledge the Artemis programme for support for radiocarbon dates at the Laboratoire de Mesure du Carbone 14. We thank Murielle Georget and Marie Hélène Castera for sample preparation and pollen extraction, Linda Rossignol for foraminifera preparation for ^{14}C dating, Ludovic Devaux for help with the surface-sample data set, and Will Banks for English proofreading. The marine core was retrieved during the NAUSICAA oceanographic cruise (IMAGES II). This work was funded by the European Research Council grant TRACSYMBOLS no. 249587 http://tracsymbols.eu/.

Edited by: D. Fleitmann

References

Archibald, S., Scholes, R. J., Roy, D. P., Roberts, G., and Boschetti, L.: Southern African fire regimes as revealed by remote sensing, International Journal of Wildland Fire, 19, 861–878, doi:10.1071/WF10008, 2010.

Barnard, P.: Biological diversity in Namibia, The Namibian National Biodiversity Task Force, Windhoek, Namibia, 332 pp., 1998.

Beal, L. M. and Bryden, H. L.: The velocity and vorticity structure of the Agulhas Current at 32° S, J. Geophys. Res.-Oceans, 104, 5151–5176, 10.1029/1998jc900056, 1999.

Beal, L. M., De Ruijter, W. P. M., Biastoch, A., and Zahn, R.: On the role of the Agulhas system in ocean circulation and climate, Nature, 472, 429–436, doi:10.1038/nature09983, 2011.

Bereiter, B., Lüthi, D., Siegrist, M., Schüpbach, S., Stocker, T. F., and Fischer, H.: Mode change of millennial CO_2 variability during the last glacial cycle associated with a bipolar marine carbon seesaw, P. Natl. Acad. Sci. USA, 109, 9755–9760, doi:10.1073/pnas.1204069109, 2012.

Bertrand, P., Balut, Y., Schneider, R., Chen, M. T., Rogers, J., and Shipboard Scientific Party: Scientific report of the NAUSICAA-IMAGES II coring cruise. Les rapports de campagne à la mer à bord du Marion-Dufresne, URA CNRS 197, Université Bordeaux1, Departement de Geologie et Oceanographie, Talence, France, 382 pp., 1996.

Bertrand, P., Giraudeau, J., Malaize, B., Martinez, P., Gallinari, M., Pedersen, T. F., Pierre, C., and Vénec-Peyré, M. T.: Occurrence of an exceptional carbonate dissolution episode during early glacial isotope stage 6 in the Southeastern Atlantic, Mar. Geol., 180, 235–248, doi:10.1016/s0025-3227(01)00216-x, 2002.

Bertrand, P., Pedersen, T. F., Schneider, R., Shimmield, G., Lallier-Verges, E., Disnar, J. R., Massias, D., Villanueva, J., Tribovillard, N., Huc, A. Y., Giraud, X., Pierre, C., and Vénec-Peyre, M.-T.: Organic-rich sediments in ventilated deep-sea environments: Relationship to climate, sea level, and trophic changes, J. Geophys. Res., 108, 3045, doi:10.1029/2000JC000327, 2003.

Biastoch, A., Böning, C. W., and Lutjeharms, J. R. E.: Agulhas leakage dynamics affects decadal variability in Atlantic overturning circulation, Nature, 456, 489–492, 2008.

Chase, B. M. and Meadows, M. E.: Late Quaternary dynamics of southern Africa's winter rainfall zone, Earth-Sci. Rev., 84, 103–138, doi:10.1016/j.earscirev.2007.06.002, 2007.

Chen, M.-T., Chang, Y.-P., Chang, C.-C., Wang, L.-W., Wang, C.-H., and Yu, E.-F.: Late Quaternary sea-surface temperature variations in the southeast Atlantic: a planktic foraminifer faunal record of the past 600 000 yr (IMAGES II MD962085), Mar. Geol., 180, 163–181, doi:10.1016/s0025-3227(01)00212-2, 2002.

Collins, J. A., Schefuß, E., Govin, A., Mulitza, S., and Tiedemann, R.: Insolation and glacial–interglacial control on southwestern African hydroclimate over the past 140 000 years, Earth Planet. Sc. Lett., 398, 1–10, doi:10.1016/j.epsl.2014.04.034, 2014.

Correa-Metrio, A., Urrego, D. H., Cabrera, K., and Bush, M. B.: paleoMAS: paleoecological analysis, R package version 1.1 Edn., 2010.

Cowling, R. M., Esler, K. J., Midgley, G. F., and Honig, M. A.: Plant functional diversity, species diversity and climate in arid and semi-arid southern Africa, J. Arid Environ., 27, 141–158, 1994.

Cowling, R. M., Richardson, D. M., and Mustart, P. J.: Fynbos, in: Vegetation of Southern Africa, edited by: Cowling, R. M., Richardson, D. M., and Pierce, S. M., Cambridge University Press, Cambridge, UK, 99–130, 1997a.

Cowling, R. M., Richardson, D. M., and Pierce, S. M.: Vegetation of Southern Africa, Cambridge University Press, Cambridge, UK, 615 pp., 1997b.

Cowling, R. M. and Hilton-Taylor, C.: Phytogeography, flora and endemism, in: The Karoo. Ecological Patterns and Processes, edited by: Dean, W. R. J., and Milton, S., Cambridge University Press, Cambridge, UK, 42–56, 2009.

Daniau, A.-L., Sánchez Goñi, M. F., Martinez, P., Urrego, D. H., Bout-Roumazeilles, V., Desprat, S., and Marlon, J. R.: Orbital-scale climate forcing of grassland burning in southern Africa, P. Natl. Acad. Sci., 110, 5069–5073, doi:10.1073/pnas.1214292110, 2013.

Dewar, G., Reimer, P. J., Sealy, J., and Woodborne, S.: Late-Holocene marine radiocarbon reservoir correction (ΔR) for the west coast of South Africa, The Holocene, 22, 1481–1489, doi:10.1177/0959683612449755, 2012.

Drysdale, R. N., Zanchetta, G., Hellstrom, J. C., Fallick, A. E., McDonald, J., and Cartwright, I.: Stalagmite evidence for the precise timing of North Atlantic cold events during the early last glacial, Geology, 35, 77–80, 2007.

Dupont, L. M.: Orbital scale vegetation change in Africa, Quaternary Sci. Rev., 30, 3589–3602, doi:10.1016/j.quascirev.2011.09.019, 2011.

Dupont, L. M. and Wyputta, U.: Reconstructing pathways of aeolian pollen transport to the marine sediments along the coastline of SW Africa, Quaternary Sci. Rev., 22, 157–174, 2003.

Dupont, L. M. and Behling, H.: Land–sea linkages during deglaciation: High-resolution records from the eastern Atlantic off the coast of Namibia and Angola (ODP site 1078), Quatern. Int., 148, 19–28, doi:10.1016/j.quaint.2005.11.004, 2006.

Dupont, L. M., Behling, H., Jahns, S., Marret, F., and Kim, J.-H.: Variability in glacial and Holocene marine pollen records offshore from west southern Africa, Veg. Hist. Archaeobot., 16, 87–100, doi:10.1007/s00334-006-0080-8, 2007.

EPICA: One-to-one coupling of glacial climate variability in Greenland and Antarctica, Nature, 444, 195–198, doi:10.1038/nature05301, 2006.

Faegri, K. and Iversen, J.: Textbook of Pollen Analysis, 4th Edn., Wiley, Chichester, 328 pp., 1989.

Gajewski, K., Lezine, A.-M., Vincens, A., Delestan, A., and Sawada, M.: Modern climate.vegetation.pollen relations in Africa and adjacent areas, Quaternary Sci. Rev., 21, 1611–1631, 2002.

Goldblatt, P.: An Analysis of the Flora of Southern Africa: Its Characteristics, Relationships, and Orgins, Ann. Mo. Bot. Gard., 65, 369–436, doi:10.2307/2398858, 1978.

González, C. and Dupont, L. M.: Tropical salt marsh succession as sea-level indicator during Heinrich events, Quaternary Sci. Rev., 28, 939–946, doi:10.1016/j.quascirev.2008.12.023, 2009.

Govin, A., Holzwarth, U., Heslop, D., Ford Keeling, L., Zabel, M., Mulitza, S., Collins, J. A., and Chiessi, C. M.: Distribution of major elements in Atlantic surface sediments (36° N–49° S): Imprint of terrigenous input and continental weathering, Geochem. Geophy. Geosy., 13, Q01013, doi:10.1029/2011GC003785, 2012.

Henderson, G. M. and Slowey, N. C.: Evidence from U-Th dating against Northern Hemisphere forcing of the penultimate deglaciation, Nature, 404, 61–66, doi:10.1038/35003541, 2000.

Heusser, L. and Balsam, W. L.: Pollen distribution in the northeast Pacific Ocean, Quatern. Res., 7, 45–62, doi:10.1016/0033-5894(77)90013-8, 1977.

Hijmans, R. J., Cameron, S. E., Parra, J. L., Jones, P. G., and Jarvis, A.: Very high resolution interpolated climate surfaces for global land areas, Internat. J. Climatol., 25, 1965–1978, 2005.

Hooghiemstra, H., Agwu, C. O. C., and Beug, H.-J.: Pollen and spore distribution in recent marine sediments: a record of NW-African seasonal wind patterns and vegetation belts, Meteor Forschungs-Ergebnisse C, 40, 87–135, 1986.

Hooghiemstra, H., Stalling, H., Agwu, C. O. C., and Dupont, L. M.: Vegetational and climatic changes at the northern fringe of the Sahara 250,000–5000 years BP: evidence from 4 marine pollen records located between Portugal and the Canary Islands, Rev. Palaeobot. Palyno., 74, 1–53, doi:10.1016/0034-6667(92)90137-6, 1992.

Hughen, K., Baillie, M., Bard, E., Bayliss, A., Beck, J., Bertrand, C., Blackwell, P., Buck, C., Burr, G., Cutler, K., Damon, P., Edwards, R., Fairbanks, R., Friedrich, M., Guilderson, T., Kromer, B., McCormac, F., Manning, S., Ramsey, C. B., Reimer, P., Reimer, R., Remmele, S., Southon, J., Stuiver, M., Talamo, S., Taylor, F., Plicht, J. V. D., and Weyhenmeyer, C.: Marine04 Marine radiocarbon age calibration, 26–0 ka BP, Radiocarbon, 46, 1059–1086, 2004.

Huntley, B., Midgley, G. F., Barnard, P., and Valdes, P. J.: Suborbital climatic variability and centres of biological diversity in the Cape region of southern Africa, J. Biogeogr., 41, 1338–1351, 2014.

Imhoff, M. L., Bounoua, L., Ricketts, T., Loucks, C., Harriss, R., and Lawrence, W. T.: Global patterns in human consumption of net primary production, Nature, 429, 870–873, 2004.

IPCC: Fifth Assessment Report of the Intergovernmental Panel on Climate Change, Intergovernmental Panel on Climate Change, NJ, USA, 2014.

Jürgens, N., Burke, A., Seely, M. K., and Jacobson, K. M.: Desert, in: Vegetation of Southern Africa, edited by: Cowling, R. M., Richardson, D. M., and Pierce, S. M., Cambridge Unversity Press, Cambridge, 189–214, 1997.

Kirst, G. J., Schneider, R. R., Müller, P. J., von Storch, I., and Wefer, G.: Late Quaternary temperature variability in the Benguela Current System derived from alkenones, Quatern. Res., 52, 92–103, doi:10.1006/qres.1999.2040, 1999.

Laskar, J.: The chaotic motion of the solar system: A numerical estimate of the chaotic zones, Icarus, 88, 266–291, 1990.

Laskar, J., Robutel, P., Joutel, F., Gastineau, M., Correia, A. C. M., and Levrard, B.: A long-term numerical solution for the insolation quantities of the Earth Astronomy and Astrophysics, 428, 261–285, 2004.

Leroy, S. and Dupont, L.: Development of vegetation and continental aridity in northwestern Africa during the Late Pliocene: the pollen record of ODP site 658, Palaeogeogr. Palaeocl., 109, 295–316, doi:10.1016/0031-0182(94)90181-3, 1994.

Lézine, A. and Hooghiemstra, H.: Land-sea comparisons during the last glacial-interglacial transition: pollen records from West Tropical Africa, Palaeogeogr. Palaeocl., 79, 313–331, doi:10.1016/0031-0182(90)90025-3, 1990.

Lisiecki, L. E. and Raymo, M. E.: A Pliocene-Pleistocene stack of 57 globally distributed benthic d18O records, Paleoceanography, 20, PA1003, doi:10.1029/2004pa001071, 2005.

Lutjeharms, J. R. E. and Meeuwis, J. M.: The extent and variability of South-East Atlantic upwelling, S. Afr. J. Marine Sci., 5, 51–62, doi:10.2989/025776187784522621, 1987.

Lyle, M., Heusser, L., Ravelo, C., Yamamoto, M., Barron, J., Diffenbaugh, N. S., Herbert, T., and Andreasen, D.: Out of the tropics: the Pacific, Great Basin Lakes, and Late Pleistocene water cycle in the western United States, Science, 337, 1629–1633, 2012.

Masson-Delmotte, V., Stenni, B., Pol, K., Braconnot, P., Cattani, O., Falourd, S., Kageyama, M., Jouzel, J., Landais, A., Minster, B., Barnola, J. M., Chappellaz, J., Krinner, G., Johnsen, S., Röthlisberger, R., Hansen, J., Mikolajewicz, U., and Otto-Bliesner, B.: EPICA Dome C record of glacial and interglacial intensities, Quaternary Sci. Rev., 29, 113–128, 2010.

McCune, B. and Grace, J. B.: Analysis of ecological communities, MjM Software Design, Gleneden Beach, Oregon, 300 pp., 2002.

Meadows, M. E., Chase, B. M., and Seliane, M.: Holocene palaeoenvironments of the Cederberg and Swartruggens mountains, Western Cape, South Africa: Pollen and stable isotope evidence from hyrax dung middens, J. Arid Environ., 74, 786–793, doi:10.1016/j.jaridenv.2009.04.020, 2010.

Mills, S. C., Grab, S. W., Rea, B. R., Carr, S. J., and Farrow, A.: Shifting westerlies and precipitation patterns during the Late Pleistocene in southern Africa determined using glacier reconstruction and mass balance modelling, Quaternary Sci. Rev., 55, 145–159, doi:10.1016/j.quascirev.2012.08.012, 2012.

Milton, S. J., Yeaton, R. I., Dean, W. R. J., and Vlok, J. H. J.: Succulent karoo, in: Vegetation of Southern Africa, edited by: Cowling, R. M., Richardson, D. M., and Pierce, S. M., Cambridge University Press, Cambridge, 131–166, 1997.

Mucina, L., Rutherford, M. C., and Powrie, L. W.: Vegetation Map of South Africa, Lesotho and Swaziland, 2nd Edn., South African National Biodiversity Institute Pretoria, 2007.

O'Connor, T. G. and Bredenkamp, G. J.: Grassland, in: Vegetation of Southern Africa, edited by: Cowling, R. M., Richardson, D. M., and Pierce, S. M., Cambridge University Press, Cambridge, UK, 215–257, 1997.

Palmer, A. R. and Hoffman, M. T.: Nama-Karoo, in: Vegetation of Southern Africa, edited by: Cowling, R. M., Richardson, D. M., and Pierce, S. M., Cambridge Unversity Press, Cambridge, 167–188, 1997.

Partridge, T. C., Demenocal, P. B., Lorentz, S. A., Paiker, M. J., and Vogel, J. C.: Orbital forcing of climate over South Africa: A 200,000-year rainfall record from the pretoria saltpan, Quaternary Sci. Rev., 16, 1125–1133, doi:10.1016/S0277-3791(97)00005-X, 1997.

Peeters, F. J. C., Acheson, R., Brummer, G.-J. A., de Ruijter, W. P. M., Schneider, R. R., Ganssen, G. M., Ufkes, E., and Kroon, D.: Vigorous exchange between the Indian and Atlantic oceans at the end of the past five glacial periods, Nature, 430, 661–665, 10.1038/nature02785, 2004.

Petit, J. R., Jouzel, J., Raynaud, D., Barkov, N. I., Barnola, J.-M., Basile, I., Bender, M., and Chappellaz, J.: Climate and atmospheric history of the past 420 000 years from the Vostok ice core, Antarctica, Nature, 399, 429–436, 1999.

Pichevin, L., Martinez, P., Bertrand, P., Schneider, R., Giraudeau, J., and Emeis, K.: Nitrogen cycling on the Namibian shelf and slope over the last two climatic cycles: Local and global forcings, Paleoceanography, 20, PA2006, doi:10.1029/2004pa001001, 2005.

Reimer, P. J., Bard, E., Bayliss, A., Beck, J. W., Blackwell, P. G., Bronk Ramsey, C., Buck, C. E., Cheng, H., Edwards, R. L., Friedrich, M., Grootes, P. M., Guilderson, T. P., Haflidason, H., Hajdas, I., Hatté, C., Heaton, T. J., Hoffmann, D. L., Hogg, A. G., Hughen, K. A., Kaiser, K. F., Kromer, B., Manning, S. W., Niu, M., Reimer, R. W., Richards, D. A., Scott, E. M., Southon, J. R., Staff, R. A., Turney, C. S. M., and Plicht, J. V. D.: IntCal13 and Marine13 radiocarbon age calibration curves 0–50 000 years cal BP, Radiocarbon, 55, 1869–1887, 2013.

Rogers, J. and Rau, A. J.: Surficial sediments of the wave-dominated Orange River Delta and the adjacent continental margin off south-western Africa, Afr. J. Mar. Sci., 28, 511–524, doi:10.2989/18142320609504202, 2006.

Röthlisberger, R., Mudelsee, M., Bigler, M., de Angelis, M., Fischer, H., Hansson, M., Lambert, F., Masson-Delmotte, V., Sime, L., Udisti, R., and Wolff, E. W.: The Southern Hemisphere at glacial terminations: insights from the Dome C ice core, Clim. Past, 4, 345–356, doi:10.5194/cp-4-345-2008, 2008.

Ruddiman, W. F.: Orbital changes and climate, Quaternary Sci. Rev., 25, 3092–3112, 2006.

Rutherford, M. C.: Categorization of biomes, in: Vegetation of Southern Africa, edited by: Cowling, R. M., Richardson, D. M., and Pierce, S. M., Cambridge University Press, Cambridge, UK, 91–98, 1997.

Sánchez Goñi, M. F., Eynaud, F., Turon, J. L., and Shackleton, N. J.: High resolution palynological record off the Iberian margin: direct land-sea correlation for the Last Interglacial complex, Earth Planet. Sc. Lett., 171, 123–137, doi:10.1016/s0012-821x(99)00141-7, 1999.

Sánchez Goñi, M. F., Turon, J.-L., Eynaud, F., and Gendreau, S.: European climatic response to millennial-scale changes in the atmosphere–ocean system during the Last Glacial period, Quatern. Res., 54, 394–403, doi:10.1006/qres.2000.2176, 2000.

Sánchez Goñi, M. F., and Harrison, S. P.: Millennial-scale climate variability and vegetation changes during the Last Glacial: Concepts and terminology, Quatern. Sci. Rev., 29, 2823–2827, 2010.

Scholes, R. J.: Savanna, in: Vegetation of Southern Africa, edited by: Cowling, R. M., Richardson, D. M., and Pierce, S. M., Cambridge University Press, Cambridge, UK, 258–277, 1997.

Scott, L.: Late Quaternary fossil pollen grains from the Transvaal, South Africa, Rev. Palaeobot. Palynol., 36, 241–268, 1982.

Scott, L., Marais, E., and Brook, G. A.: Fossil hyrax dung and evidence of Late Pleistocene and Holocene vegetation types in the Namib Desert, J. Quaternary Sci., 19, 829–832, doi:10.1002/jqs.870, 2004.

Scott, L., Neumann, F. H., Brook, G. A., Bousman, C. B., Norström, E., and Metwally, A. A.: Terrestrial fossil-pollen evidence of climate change during the last 26 thousand years in Southern Africa, Quaternary Sci. Rev., 32, 100–118, doi:10.1016/j.quascirev.2011.11.010, 2012.

Shi, N., Dupont, L. M., Beug, H.-J., and Schneider, R.: Correlation between vegetation in southwestern Africa and oceanic upwelling in the past 21,000 years, Quatern. Res., 54, 72–80, doi:10.1006/qres.2000.2145, 2000.

Shi, N., Schneider, R., Beug, H.-J., and Dupont, L. M.: Southeast trade wind variations during the last 135 kyr: evidence from pollen spectra in eastern South Atlantic sediments, Earth Planet. Sc. Lett., 187, 311–321, doi:10.1016/s0012-821x(01)00267-9, 2001.

Southon, J., Kashgarian, M., Fontugne, M., Metivier, B., and Yim, W. W.-S.: Marine reservoir corrections for the Indian Ocean and Southeast Asia, Radiocarbon, 44, 167–180, 2002.

Stuut, J.-B. W., Prins, M. A., Schneider, R. R., Weltje, G. J., Jansen, J. H. F., and Postma, G.: A 300-kyr record of aridity and wind strength in southwestern Africa: inferences from grain-size distributions of sediments on Walvis Ridge, SE Atlantic, Mar. Geol., 180, 221–233, doi:10.1016/s0025-3227(01)00215-8, 2002.

Stuut, J.-B. W. and Lamy, F.: Climate variability at the southern boundaries of the Namib (southwestern Africa) and Atacama (northern Chile) coastal deserts during the last 120,000 yr, Quatern. Res., 62, 301–309, doi:10.1016/j.yqres.2004.08.001, 2004.

Toggweiler, J. R. and Russell, J.: Ocean circulation in a warming climate, Nature, 451, 286–288, 2008.

Tyson, P. D.: Atmospheric circulation changes and palaeoclimates of southern Africa, S. Afr. J. Sci., 95, 194–201, 1999.

Tyson, P. D. and Preston-Whyte, R. A.: The weather and climate of southern Africa, Oxford University Press Southern Africa, Cape Town, 396 pp., 2000.

Waelbroeck, C., Frank, N., Jouzel, J., Parrenin, F., Masson-Delmotte, V., and Genty, D.: Transferring radiometric dating of the last interglacial sea level high stand to marine and ice core records, Earth Planet. Sc. Lett., 265, 183–194, 2008.

Wang, X., Auler, A. S., Edwards, R. L., Cheng, H., Cristalli, P. S., Smart, P. L., Richards, D. A., and Shen, C.-C.: Wet periods in northeastern Brazil over the past 210 kyr linked to distant climate anomalies, Nature, 432, 740–743, 2004.

Weldeab, S., Stuut, J.-B. W., Schneider, R. R., and Siebel, W.: Holocene climate variability in the winter rainfall zone of South Africa, Clim. Past, 9, 2347–2364, doi:10.5194/cp-9-2347-2013, 2013.

White, F.: The vegetation of Africa: a descriptive memoir to accompany the Unesco/AETFAT/UNSO vegetation map of Africa, Paris, 356 pp., 1983.

Woillez, M.-N., Levavasseur, G., Daniau, A.-L., Kageyama, M., Urrego, D. H., Sánchez-Goñi, M.-F., and Hanquiez, V.: Impact of precession on the climate, vegetation and fire activity in southern Africa during MIS4, Clim. Past, 10, 1165–1182, doi:10.5194/cp-10-1165-2014, 2014.